Predicting NOx Emissions in Diesel Engines via Sigmoid NARX Models Using A New Experiment Design for Combustion Identification

Gokhan Alcan[a,b], Mustafa Unel[a,b,*], Volkan Aran[a,c],
Metin Yilmaz[c], Cetin Gurel[c], Kerem Koprubasi[c]

[a] *Faculty of Engineering and Natural Sciences, Sabanci University, Istanbul, Turkey*
[b] *Integrated Manufacturing Technologies Research and Application Center, Sabanci University, Istanbul, Turkey*
[c] *Product Development, Ford Otosan, Istanbul, Turkey*

Abstract

Diesel engines are still widely used in heavy-duty engine industry because of their high energy conversion efficiency. In recent decades, governmental institutions limit the maximum acceptable hazardous emissions of diesel engines by stringent international regulations, which enforces engine manufacturers to find a solution for reducing the emissions while keeping the power requirements. A reliable model of the diesel engine combustion process can be quite useful to search for the best engine operating conditions. In this study, nonlinear modeling of a heavy-duty diesel engine NOx emission formation is presented. As a new experiment design, air-path and fuel-path input channels were excited by chirp signals where the frequency profile of each channel is different in terms of the number and the direction of the sweeps. This method is proposed as an alternative to the steady-state experiment design based modeling approach to substantially reduce testing time and improve modeling accuracy in transient operating conditions. Sigmoid based nonlinear autoregressive with exogenous input (NARX) model is employed to predict NOx emissions with given input set under both steady-state and transient cycles. Models for different values of parameters are generated to analyze the sensitivity to parameter changes and a parameter selection method using an easy-to-interpret map is proposed to find the best modeling parameters. Experimental results show that the steady-state and the transient validation accuracies for the majority of the obtained models are higher than 80% and 70%, respectively.

Keywords: Diesel Engine, Combustion Process, NOx Emissions, Experiment Design, Sigmoid NARX Model

*Corresponding author. *E-mail*: munel@sabanciuniv.edu

1. Introduction

Increasingly tightened NOx emission regulations limit the maximum acceptable emission values, which pushes engine manufacturers to make innovations by introducing aftertreatment systems [1] or combustion control techniques [2] to reduce NOx emissions of diesel engines. In addition to precautions for pollutant emissions, increasing fuel prices and the demand for more powerful engines lead engine and vehicle manufacturers to search for the optimum engine operating conditions. To be able to exploit the remaining potential of reducing the emissions and increasing the power, obtaining sufficiently accurate models of the diesel engine combustion process in both steady-state and transient operations becomes very critical. Once a reliable model of the engine process including combustion and emission formation is obtained, it can be employed in powertrain development for the optimization of engine components, development, testing and model-based calibration of combustion and aftertreatment control [3].

Existing studies on diesel engine NOx emission modeling can be investigated in three groups based on the level of available information such as white, grey and black box modeling [4]. When the system's dynamics are fully known or can be derived by employing physical or phenomenological laws, the identification process is called white box [5, 6, 7]. In that case, only the parameter values of the system are estimated with experimental data. In grey box modeling, a combination of partial knowledge of the system dynamics and the experimental measurements constitute a model [8, 9, 10, 11]. Finally, in black box modeling, no knowledge regarding the dynamics of the system is utilized and the models are derived by performing experiments.

Combustion and NOx emission formation in a diesel engine are highly nonlinear and complex processes, so white or grey box models do not have enough generalization capabilities due to assumptions and simplifications. Therefore, purely data-driven approaches are widely employed in such cases. Benatzky et al. [12] presented the design and evaluation of NOx models for heavy-duty off-road engines by using static polynomial black-box modeling. They investigate three approaches, differing in the chosen sets of regressors such as the input signals available on a standard electronic control unit (ECU approach), engine speed and the features extracted from the in-cylinder pressure trace by singular value decomposition (SVD

approach), and finally the geometric values from the pressure trace and heat release curves (HRL approach). Although validation performance of each individual approach is unsatisfactory, their combination provides quite satisfactory validation results. However, authors also reported that relatively large deviations may occur between the model predictions and the measurements for higher NOx values depending on the sudden changes in engine speed. Henningsson et al. [13] presented a linear state-space model for the dynamics of a six-cylinder heavy-duty engine over a range of operating points. Fuel injection duration, fuel injection timing, exhaust gas recirculation (EGR) and variable geometry turbo (VGT) are considered as inputs, indicated mean effective pressure, combustion phasing, peak pressure derivative, NOx and soot emissions are modeled as outputs. Wiener models are introduced to reduce the number of local linear models at each operating point. Authors employed linear methods to obtain appropriate local models for model-based control design, but it could decrease the prediction performance in transient cycles which was not validated in the study. Grahn et al. [14] described the model structures for NOx and soot emissions of a 5-cylinder Volvo passenger car diesel engine as local linear regression models where the regression parameters are defined by two-dimensional look-up tables. Then they interpreted them as a B-spline function and showed how the globally optimal model parameters could be found by solving a linear least-squares problem. Proposed method predicts the NOx mass flow with an average relative error of 5.1% under steady-state engine operation, but the prediction performance during transient cycles is still needed to be verified. Formentin et al. [15] utilized engine speed and indicated pressure measurements to estimate NOx emissions of a heavy-duty diesel engine. They used principal component analysis and L2 regularization technique to derive a reliable and straightforward estimator. Authors reported that their method is targetted to aftertreatment and closed-loop combustion control. Therefore the estimation performance is quite satisfactory with 0.48% normalized mean estimation error whenever the static assumption holds, but it is not guaranteed to predict transient peaks precisely. Boz et al. [16] developed a novel input design framework in terms of multi-sweep chirp signals, and airpath input channels are excited by those signals. Next, they compared the capabilities of linear and nonlinear system identification models for a diesel engine NOx emission and showed the superiority of nonlinear autoregressive with exogenous input (NARX) models for such highly

nonlinear process. In that work, only airpath input channels were employed in modeling and up to 80% steady-state validation accuracy was achieved. Roy et al. [17] employed an artificial neural network structure (ANN) to estimate BSFC, BTE, CO2, NOx and PM emissions of a Common Rail Diesel Injection (CRDI) type engine. In that work, they considered load, fuel injection pressure, EGR and fuel injected per cycle as inputs for the network. Their method performs well with noticeably low root mean square errors in NOx predictions under steady-state cycles. However the prediction performance of their modeling structure under transient cycles could be problematic since the ANN structure is inadequate to capture the dynamic relations between inputs and outputs.

In this paper, data-driven modeling of diesel engine NOx emission formation using sigmoid based nonlinear autoregressive with exogenous input (NARX) model is presented. To generate data for training these models, two separate experiments with different input designs based on chirp and ramp-hold signals are conducted and then merged to cover both steady-state and transient cycles of the combustion process. With the proposed experiment design, it is targeted to reduce testing time dramatically and improve modeling accuracy in both steady-state and transient operating conditions as an alternative to the steady-state DoE based modeling approaches. A single layer sigmoid NARX model with various number of neurons has been designed to model NOx emissions. A sensitivity analysis for model parameters is conducted by generating models for different values of parameters selected from prespecified ranges. In order to select the most suitable parameters for diesel engine emissions modeling with limited testing time in powertrain development, an easy-to-interpret map which employs the 3D surface plots of the best fit model performances including training and validation is proposed as a convenient means. Results of the experiments show that the steady-state and transient validation accuracies for 80% of the obtained models are higher than 80% and 70%, respectively. Moreover, the training fit accuracies of all models were higher than 70% and it was higher than 80% for an overwhelming majority. The first draft of this study has appeared in [18].

The organization of this paper is as follows: Diesel engine combustion and the experimental setup are briefly described in Section 2. A new experiment design is proposed in Section 3. Sigmoid NARX model is provided in Section 4. Experimental results with sensitivity analysis

and parameter selection method are presented in Section 5. Finally, the paper is concluded with some remarks in Section 6.

2. Overview of NOx Emissions and Control in Diesel Engines

Increasingly stringent emission regulations are driving the evolution of internal combustion engine technologies. Especially NOx emissions are a focal point in the advancement of a diesel engine and aftertreatment technologies, influencing overall vehicle development and hardware costs together with many other important vehicle attributes. There is a trade-off between NOx emissions, soot emissions, and fuel economy from an engine calibration standpoint. Accurate prediction of NOx emissions is critical for fuel economy optimization in diesel engines.

2.1. European Emission Regulations

As the pollutant emission limits become more stringent, regulation test cycles also become more dynamic in nature. For heavy-duty vehicles in Europe, the World Harmonized Transient Cycle (WHTC) replaced the European Transient Cycle (ETC) with the introduction of Euro 6 regulations, featuring more dynamic characteristics compared to its predecessor. For light-duty commercial vehicles and passenger cars in Europe, Worldwide Light-duty Test Cycle (WLTC) replaces the New European Driving Cycle (NEDC) test with the introduction of Euro 6.2 regulations [19]. WLTC includes more transient maneuvers in contrast to NEDC, where the vehicle is mostly driven in steady state conditions. WLTC also covers a much wider engine operating range, which includes the full load region. On-road emission tests are also implemented for heavy duty (Euro VI onward), light duty and passenger car (Euro 6b onward) vehicles. In-service conformity (ISC) and Real Drive Emissions (RDE) on-road emission tests are required using Portable Emission Measurement System (PEMS) and they feature highly dynamic characteristics due to real-world driving conditions. The dynamic nature of WHTC, WLTP, RDE, and PEMS test cycles increases the emphasis of transient operation in terms of combustion optimization [20]. Therefore, accurate modeling of transient NOx emissions is a key enabler for offline optimization, online control and onboard diagnostic of diesel engine combustion considering future diesel engine technologies [21].

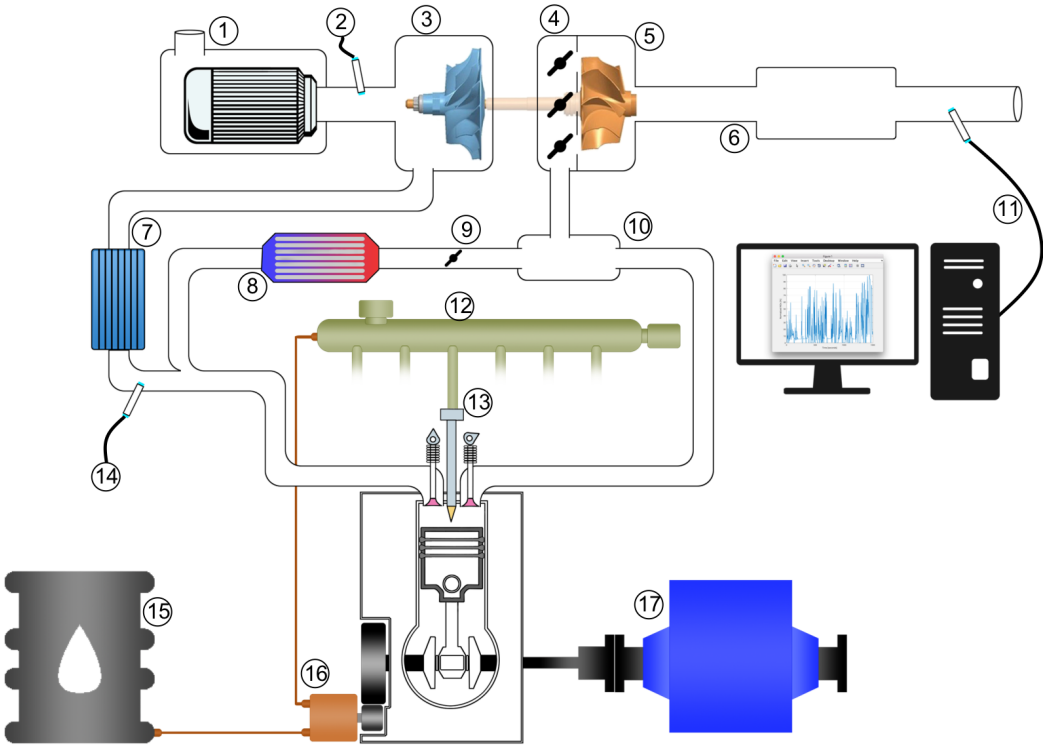

Figure 1: Schematic of experimental setup: (1) Air filter, (2) MAF sensor, (3) Compressor, (4) Turbine, (5) VGT, (6) Exhaust pipe, (7) Charge air cooler, (8) EGR cooler, (9) EGR valve, (10) Exhaust manifold, (11) Exhaust gas measurement system, (12) Pressurized rail, (13) Injector, (14) TMAP sensor, (15) Fuel tank, (16) High pressure fuel pump, (17) AVL Dynamometer

2.2. Physical System Description

The Ecotorq 13L Euro 6 engine has high-pressure EGR routing and swing vane variable geometry turbocharger on the air path as depicted in Figure 1. The common fuel rail, solenoid injectors and high-pressure fuel pump are elements of the fuel system. Fresh air coming from the ambient flows through an air filter and is measured before the compressor. This air flow measurement is referred to as Mass Air Flow (MAF). The compressor section of the turbocharger increases the pressure of induced air to a regulated level. Charge air cooler reduces the compressed air temperature in order to increase the volumetric efficiency of the engine. Temperature and pressure of the cooled charge air are measured before the EGR mixing point. The pressure at the charge air cooler and intake valves are assumed to be approximately equal and it is called Manifold Air Pressure (MAP). Exhaust gases from previous combustion cycles are fed into the intake line through EGR cooler. EGR is utilized in order to decrease the O_2 concentration of air while keeping the same MAP. Another effect

Type	: Ecotorq 12.7 lt.	Cylinder Bore	: 130 mm
Power	: 480 PS (353 kW) /1800 d/d	Cylinder Stroke	: 160 mm
Torque	: 2500 Nm/1000-1200 d/d	Turbocharger	: VGT
Compression Ratio	: 17 $\pm$ 0.5 : 1	EGR	: High Pressure, Cooled
Cylinders	: 6 in line	Fuel System	: Common Rail
Cylinder Volume	: 12740 cc	Rail Pressure	: Max. 2500 bar

Table 1: Test engine spesifications

of the EGR is increasing the heat capacity of the air mixture. EGR and fresh air mixture are sucked into the engine through the intake ports (i.e. 2 intake valves per cylinder) during the intake stroke. Compression stroke increases the pressure and temperature of the air-EGR mixture due to a volume change. Main and pilot fuel injectors are electronically controlled and the start of injection (SOI) and duration of energizing can be controlled as a function of the crank angle. Additionally, the common rail pressure is regulated via the injection pump metering unit and pressure control valves. Diesel fuel is injected at a certain pressure, timing and duration to the compressed hot air-EGR mixture and combustion take place. A certain portion of the exhaust gases is directed to the inlet and its mass flow is regulated by the EGR valve. The remaining exhaust gases are directed to the turbine wheel via swing vanes. By controlling vane swing angle, inlet angle and speed of the exhaust gas to the turbine are regulated. Turbochargers with this type of actuators are called Variable Geometry Turbine (VGT) turbochargers. The exhaust gas expanded in the turbine is sent to the exhaust line and its chemical composition is measured by the exhaust gas measurement system. Specifications of the test engine are listed in Table 1.

2.3. NOx Formation and Control Mechanisms

Formation of NOx is a nonlinear process and it is influenced by many parameters, most important of which are in-cylinder combustion temperature and amount of oxygen in the cylinders [22]. Mainstream NOx control methods used for the diesel engines focus on reducing these parameters, however, these control actions have an adverse effect on fuel economy. Calibration parameters to control the combustion process of a typical common rail diesel engine with EGR system can be divided into two groups, related to fuel path and air path

systems. Most significant fuel path calibration parameters for NOx control are start of main injection, main injection fuel quantity and fuel pressure at common rail.

Advancing the SOI of main injection increases the peak combustion temperature, improving combustion efficiency while increasing NOx emissions. The fuel quantity of the main injection also increases the combustion temperature, therefore, increasing NOx emissions. Incrementing common rail fuel pressure increases heat release during the pre-mixed combustion phase and therefore peak firing temperatures. While rail fuel pressure improves combustion efficiency and reduces soot emissions due to better mixing of air and fuel, it also increases NOx emissions significantly.

3. Experiment Design

Design of experiments includes the selection of model inputs, the selection of excitation signals and the selection of validation signals. In this work, input set involves the signals from both fuel and air paths of a diesel engine. Within this context, engine speed (SPD), Manifold Absolute Pressure (MAP), Mass Air Flow (MAF), rail pressure (railP), main and pilot injection fuel quantities (miQNT and piQNT), main and pilot start of injections (miSOI and piSOI) are chosen as input channels for NOx emission model shown in Figure 2.

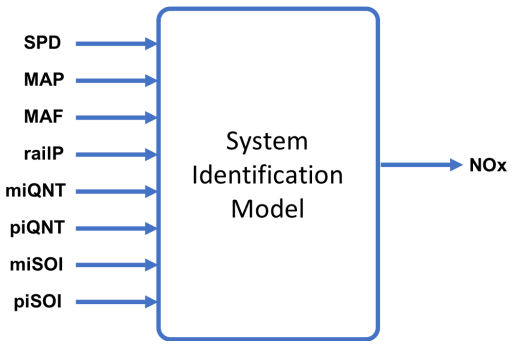

Figure 2: Inputs and output for system identification model

Here the EGR value is indirectly taken into consideration using MAF and MAP setpoints. EGR valve control is enabled for the entire duration of the tests to meet the MAF setpoint, and MAP is controlled using the turbocharger (VGT) actuator. Since MAP directly determines the amount of total gas flow into the engine considering volumetric efficiency; the difference between total gas flow and MAF is equal to the actual EGR flow into the engine. The

rationale for using MAF and MAP as reference signals instead of valve positions is to be able to cover a more realistic engine operating range in terms of air-fuel ratio (AFR) and EGR flow. EGR ratio coverage is also monitored after the tests to ensure that we achieve informative experiments in terms of magnitude coverage.

Design of excitation signals plays a decisive role in the parameter estimation and the achievable model validation performances. Typically, model-based and model-free approaches are employed in excitation signal design based on the available information about the underlying process [23]. Design of excitation signals in model-based approaches utilizes a prior model of the process to adjust the signals specifically to the system [24]. On the other hand, model-free approaches necessitate to cover the whole intended input space by using space filling methods [25]. Moreover, the excitation signals for dynamic systems should also encapsulate the frequency range of underlying process [26]. Therefore, chirp signals are commonly preferred in the identification of nonlinear dynamic systems because of their persistent excitation capabilities. Furthermore, they have lower crest factor (1), which indicates that they inject much more power into the system than the signals having the same peak value and a higher crest factor [27].

$$C_r^2 = \frac{max_t u^2(k)}{\lim\limits_{N\to\infty} \frac{1}{N} \sum\limits_{k=1}^{n} u^2(k)} \tag{1}$$

NOx formation of a diesel engine is considered to have a nonlinear complex dynamic nature that requires to have a model-free design of excitation signals. Because of aforementioned advantages of periodic signals, input channels were excited by chirp signals, which have sinusoidal waveform with changing frequencies over time given by

$$y(t) = Asin(2\pi f(t)) \tag{2}$$

where the frequency of the chirp signal can be a linear, quadratic or an exponential function of time. The models obtained within the scope of this work are aimed to be validated in both steady-state and transient cycles. Therefore, in order to excite the system adequately in both high and low frequencies, a quadratic function is employed as

$$f(t) = f_{min} + \Big(\frac{f_{max} - f_{min}}{t_{max}^2}\Big) t^2 \tag{3}$$

where f_{max} is the maximum frequency (0.25 Hz), f_{min} is the minimum frequency (0.01 Hz) and

t_{max} is the time that the system operates at maximum frequency. The frequency range of the input signals is determined by investigating the World Harmonic Transient Cycle (WHTC) [28] and New European Driving Cycle (NEDC) [29]. Engine control unit software contains a mechanism that enables to manipulate the setpoints of the input channels. For example, in normal ECU operation, all combustion setpoints are calculated using 2-D look-up tables which are dependent on engine speed and indicated engine torque. However, in our test scenario, the outputs of these 2-D look-up tables are overwritten by our pre-generated setpoint values. We can set these override values from MATLAB using the API of the ECU calibration software (ATI Vision) during the dynamometer tests to be able to vary the frequency of input signals independent of engine speed.

In the identification of multi-input systems, it is very critical to have low correlation between input signals to obtain maximum informative experiments. In order to decouple the input channels, the number and the directions of the sweeps in frequency profiles of the chirp signals are selected differently. The number of forward sweeps is increased in the frequency profiles of SPD, MAF, miSOI and piQNT, respectively. In the same way, reversed sweeps are applied for miQNT, MAP, railP and piSOI, respectively. Short-time Fourier transform of the designed input signals depicts the frequency profiles of the inputs in Figure 3.

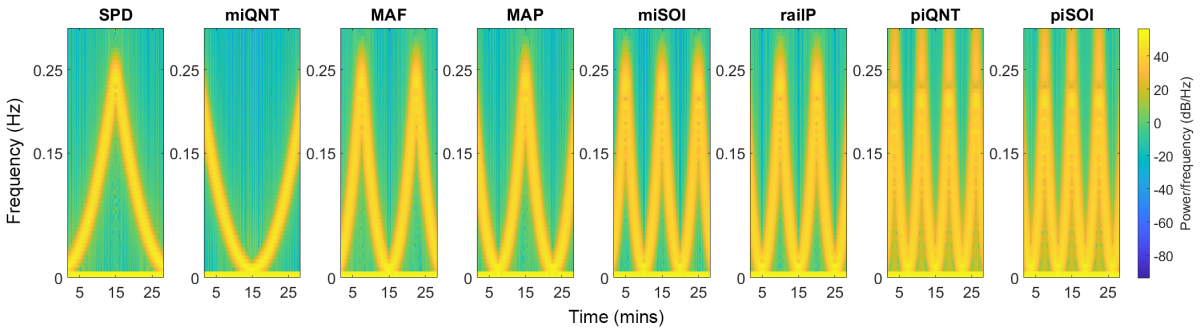

Figure 3: Frequency profiles of input channels

In order to check the correlation between input channels, Pearson coefficient for pair-wise channels is calculated as follows and presented in Table 2.

$$\gamma = \frac{| < x - \bar{x}, y - \bar{y} > |}{\|x - \bar{x}\| \|y - \bar{y}\|} \tag{4}$$

Pearson coefficient is 0 when two signals are completely different and 1 when the signals have maximum similarity. Table 2 shows that the desired input signals are sufficiently

	SPD	MAP	MAF	railP	miQNT	piQNT	miSOI	piSOI
SPD	1	0.050	0.092	0.017	0.033	0.004	0.085	0.050
MAP	0.050	1	0.046	0.003	0.050	0.057	0.003	0.022
MAF	0.092	0.046	1	0.108	0.092	0.057	0.108	0.022
railP	0.017	0.003	0.108	1	0.085	0.065	0.057	0.025
miQNT	0.033	0.050	0.092	0.085	1	0.004	0.017	0.050
piQNT	0.004	0.057	0.057	0.065	0.004	1	0.065	0.082
miSOI	0.085	0.003	0.108	0.057	0.017	0.065	1	0.025
piSOI	0.050	0.022	0.022	0.025	0.050	0.082	0.025	1

Table 2: Correlations between designed input signals

decoupled, since all the coefficients for pair-wise different channels are less than 0.1.

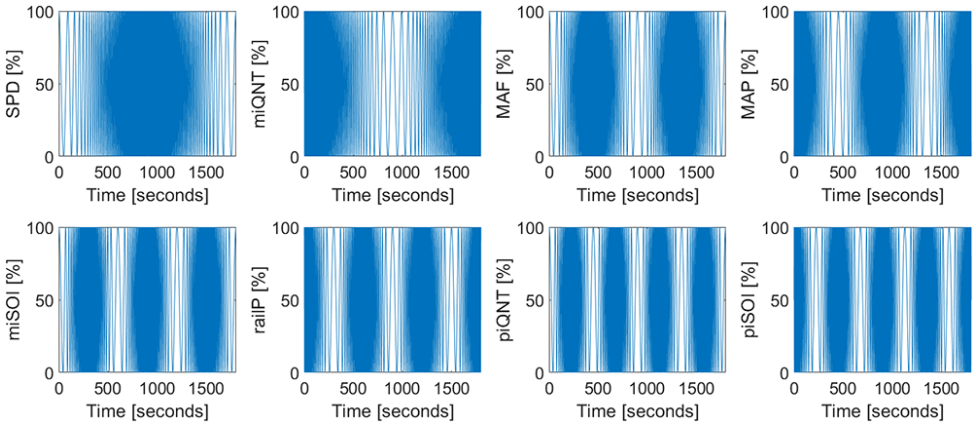

Figure 4: Normalized input signals (Experiment 1)

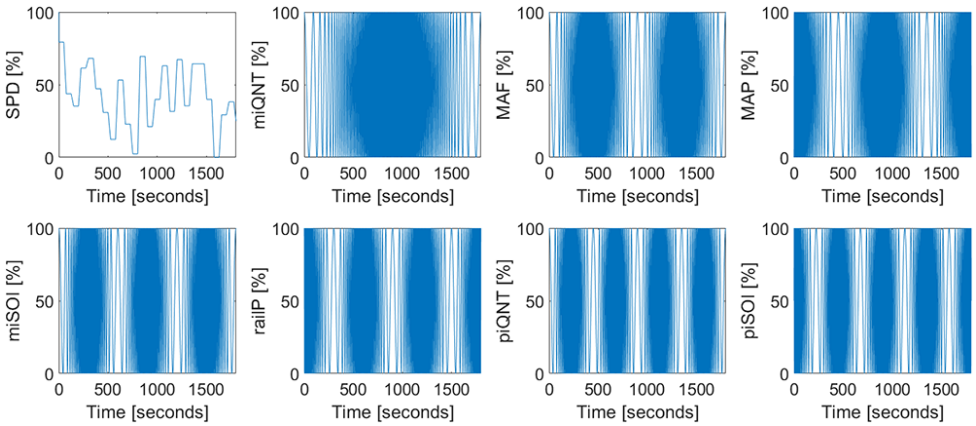

Figure 5: Normalized input signals (Experiment 2)

In order to increase the prediction accuracy in the steady-state cycle of diesel engine

NOx emission formation, an additional experiment with different excitation signals for engine speed and main injection fuel quantity were designed. Different from the first experiment, engine speed was excited by a ramp-hold signal at different levels and the frequency profile of the main injection fuel quantity channel was changed to a single forward sweep. By doing so, it was targeted that the speed - fuel quantity operation region in Experiment 2 contains much lower frequencies than Experiment 1. Duration of each experiment was 30 minutes and the signals were collected in 10 Hz. Both experiments were merged and employed in the training. Normalized input signals for NOx emissions are shown in Figure 4 and 5 for reasons of confidentiality.

4. System Identification

Diesel engine combustion and NOx emission formation are highly complex dynamic processes. Boz et al. [16] showed that the linear models are not sufficient to represent the nature of NOx emission formation and nonlinear models perform better in validation tests compared to linear ones. Therefore, a single layer recurrent nonlinear autoregressive with exogenous input (NARX) model was selected as modeling structure and it can be expressed as

$$y(k) = w_0 x(k) + b_0 + \sum_{i=1}^{m} \phi_i (w_i x(k) + b_i) + e(k) \tag{5}$$

where $y(k)$ is the output, $x(k)$ is the regressor set, w_i and b_i are the weights and bias parameters of the nonlinear part, w_0 and b_0 are the weights and bias parameters of the linear part, ϕ_i is the nonlinear activation function, m is the number of units used in the hidden layer and $e(k)$ is the modeling error.

Regressor set consists of the past values of inputs and output. It is experimentally verified that using the increasing number of output regressors results in the divergence of the optimization algorithm very frequently during the parameter estimation process. Therefore, a single past value of the output is included in the regressor set.

Nonlinear activation function (ϕ) is selected as a sigmoid function that can be written as

$$\sigma(x) = \frac{1}{1 + e^{-ax}} \tag{6}$$

where a is a positive parameter to be estimated as well. The schematic of the sigmoid NARX model is presented in Figure 6. The parameter d shown in Figure 6 is the pure time delay

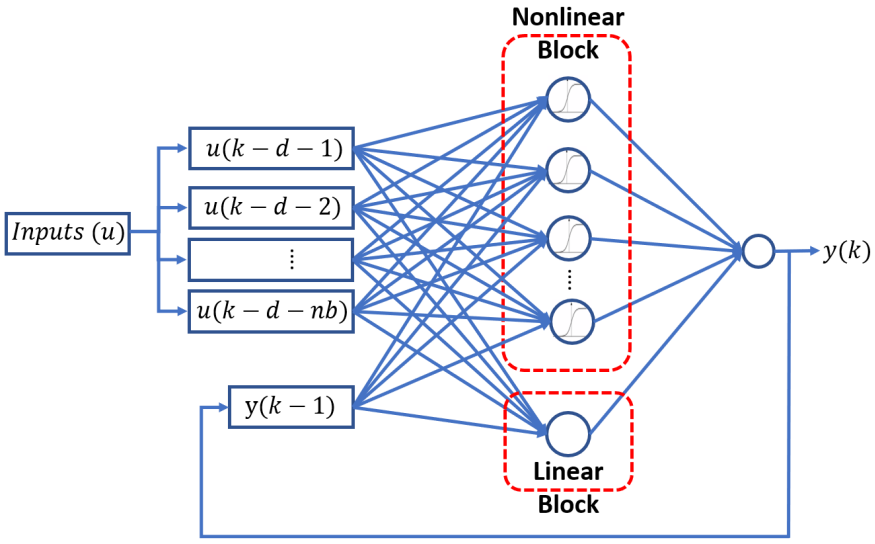

Figure 6: Sigmoid NARX model structure

between inputs and output. Since the system can not respond instantaneously when the inputs are applied, the pure time delay should be at least 1 sample. In this work pure time delay was determined as 3.5 seconds (35 samples) due to the physical distances between the sensors.

The parameters in the sigmoid NARX model are estimated iteratively by using a combination of the line search algorithms such as subspace Gauss-Newton least squares search, Levenberg-Marquardt least squares search, adaptive subspace Gauss-Newton search and steepest descent least squares search [30].

5. Sensitivity Analysis and Parameter Selection

To investigate the training and the validation performances, models for the ranges of parameters given in Table 3 were generated. The input regressor number and the unit number are the parameters of the model structure, whereas the maximum number of bisections used for line search along the search direction and the iteration number are the parameters of the optimization algorithm.

It should be noted that equal number of regressors are taken from each input channel. During the parameter estimation process, optimization algorithm searches for the best set of parameters that minimizes the error between the predicted and the measured output. Optimization runs for 20 iteration steps and the obtained model is evaluated with training

Parameter	Range
Input Regressor Number	3-10
Unit Number	5-15
Maximum Bisections	4-7
Iteration	20,40,60,80,100

Table 3: Ranges of parameters

and validation (both steady-state and transient) tests. The last estimated model is utilized as initial model for next estimation up to 100 iterations. By doing so, 1760 models were obtained. Once the parameters regarding the model structure (input regressor and unit numbers) are fixed, there will be 20 models due to the variation of optimization parameters. In order to assess the performances of all models and determine the best optimization parameters, scores in terms of points (P) are calculated as the weighted average of training and validation performances as follows:

$$P = \frac{1}{3}\Big(\omega_1 fit_{train} + \omega_2 fit_{NEDC} + \omega_3 fit_{WLTC}\Big) \tag{7}$$

where fit_{train} is the training fit performance, fit_{NEDC} and fit_{WLTC} are the validation performances for steady-state (NEDC) and transient (WLTC) tests, respectively. These performances are calculated by the fit metric given by

$$fit = 100 \times \Big(1 - \frac{\|y - \hat{y}\|}{\|y - \bar{y}\|}\Big) \tag{8}$$

The weights in (7) (ω_1, ω_2 and ω_3) are calculated as

$$\omega_1 = \frac{100}{max(fit_{train})}, \quad \omega_2 = \frac{100}{max(fit_{NEDC})}, \quad \omega_2 = \frac{100}{max(fit_{WLTC})} \tag{9}$$

After the determination of best optimization parameters for each pair of unit and regressor numbers, 88 different models are obtained. Distributions of training, steady-state and transient validation performances of those 88 models are depicted in Figure 7. Each slice of the pie chart represents the percentage of the models which have the fit performance in the same interval. Figure 7(a) shows that the training fit accuracies of the all models are higher than 70% and 72% of the models have the training fit accuracy between 80% and 90%. Distributions of the validation performances show that 80% of the models have the fit accuracy

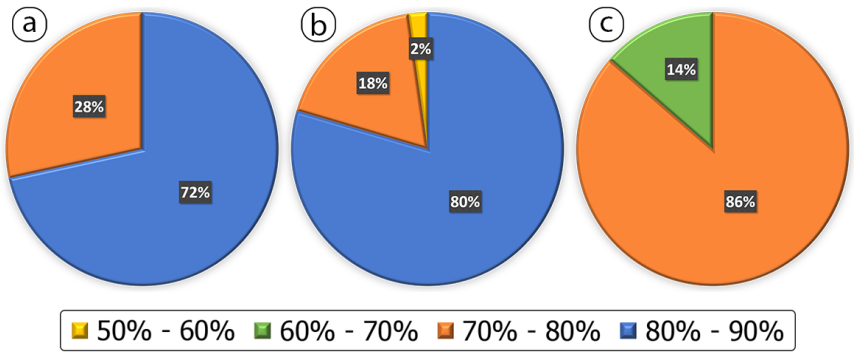

Figure 7: Distributions of (a) training, (b) steady-state validation and (c) transient validation performances

between 80% and 90% under steady-state cycles and 86% of the models have the fit accuracy between 70% and 80% under transient cycles (Figure 7(b)-(c)). It should be noted that the WLTC includes higher loads and velocity distributions than the NEDC [31], which makes it more challenging to obtain fit accuracies higher than 80% under transient cycles.

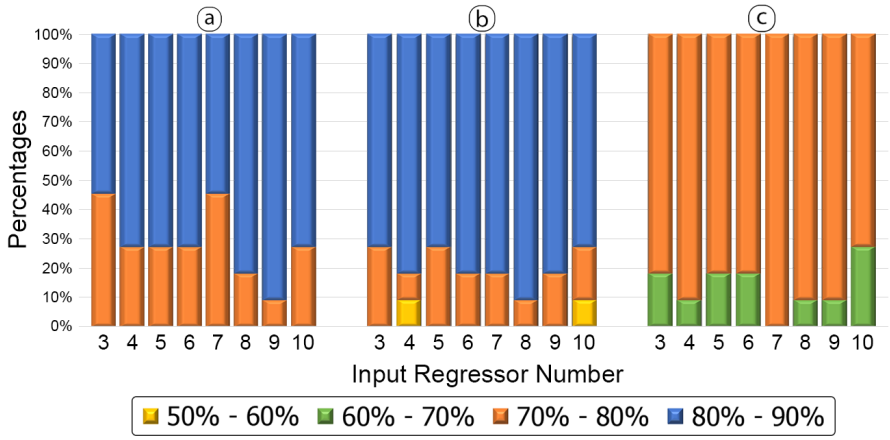

Figure 8: (a) Training, (b) steady-state and (c) transient validation performances by changing the input regressors number

Distributions of the training and the validation performances by changing the input regressor and the unit numbers are presented in Figure 8 and 9, respectively. These distributions reveal the influences of model structure parameters on the training and the validation performances. Figure 8 shows that 8 or 9 input regressors would be a reasonable choice to obtain high training and validaton accuracies. The models with at least 11 units in the hidden layer achieved the training accuracy higher than 80% (Figure 9). Furthermore, all the models with 14 or 15 units have the highest training and validaton accuracies.

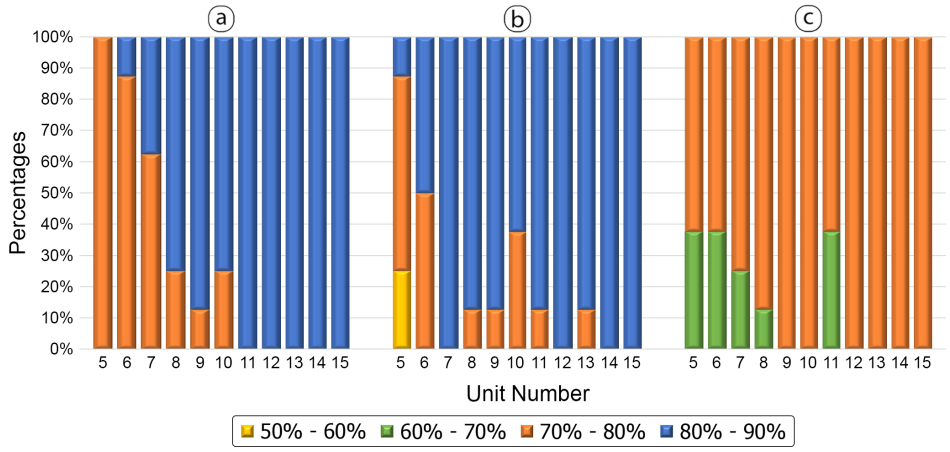

Figure 9: (a) Training, (b) steady-state and (c) transient validation performances by changing the unit number

In order to investigate the pairwise effects of model structure parameters, 3D model performances are depicted in Figure 10, where the third dimension is the best fit performance of the model and the first two dimensions are the corresponding unit and regressor numbers.

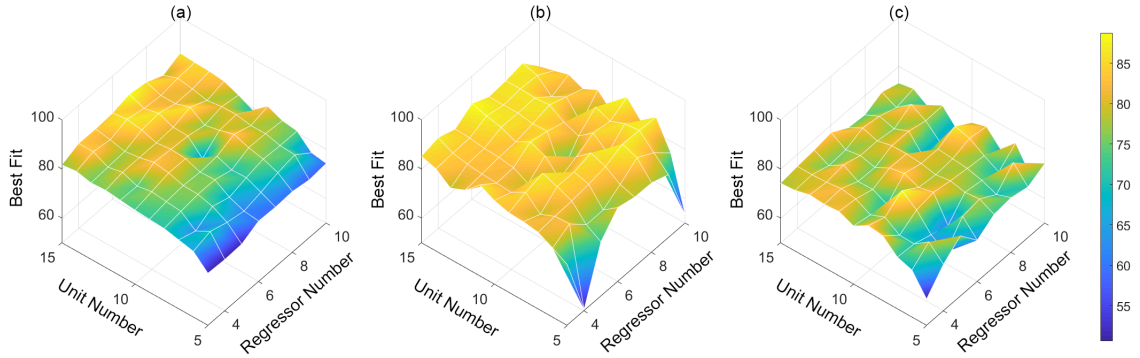

Figure 10: 3D surface plots of (a) training, (b) steady-state and (c) transient validation performances

The yellow regions represent the high fit accuracies, whereas the regions of low fit accuracies are shown in blue (Figure 10). Thus, the problem of finding a good model with high training and validation performances boils down to the searching for the peak points in the presented graphs.

Since it may not always be easy to find the best model that is valid for each graph, the points given in (7) are calculated for these models by considering their performances and a single easy-to-interpret map for parameter selection is obtained (Figure 11). Obtained map can be a convenient engineering solution to select the required parameters for diesel engine emissions modeling with limited testing time in powertrain development. It should be noted

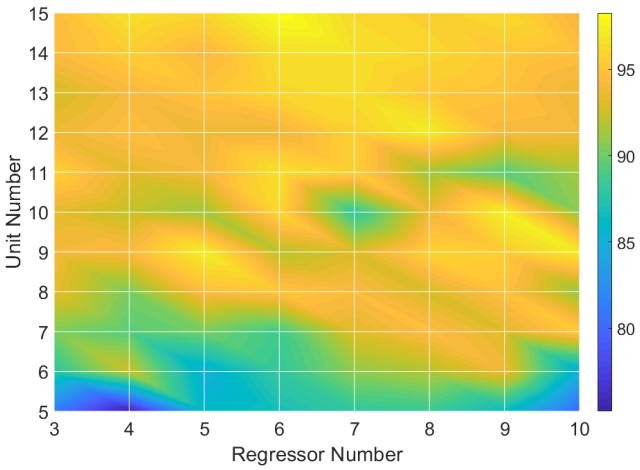

Figure 11: Obtained map for parameter selection

that the regions with similar yellow colors indicate the places of robust models with high performances. The map in Figure 11 also demonstrates the sensitivity of the models for parameter changes. For instance, it would be recommended to select the center point of a large yellow area to obtain a robust model with high validation accuracies.

Performances of some selected models by utilizing the map in Figure 11 are tabulated in Table 4. The best model according to P points (7) employs 6 input regressor number and 15 units. The model was trained by 84,92% fit accuracy, and the steady-state and the transient validation accuracies are 88,75% and 76,96%, respectively.

Regressor Number	Unit Number	Maximum Bisections	Iterations	Training (%)	NEDC (%)	WLTC (%)
6	15	5	40	84,92	88,75	76,96
5	9	4	40	81,61	86,59	79,53
8	12	5	60	85,48	86,40	75,74
7	14	7	60	84,21	85,54	76,24
9	9	4	20	82,18	83,96	77,01
5	6	7	100	76,74	75,74	64,56
4	5	6	100	70,93	50,63	68,95

Table 4: Selected model performances

In Figure 12, 13 and 14, steady-state and transient validation performances of the best three models in Table 4 are demonstrated in time plots, respectively.

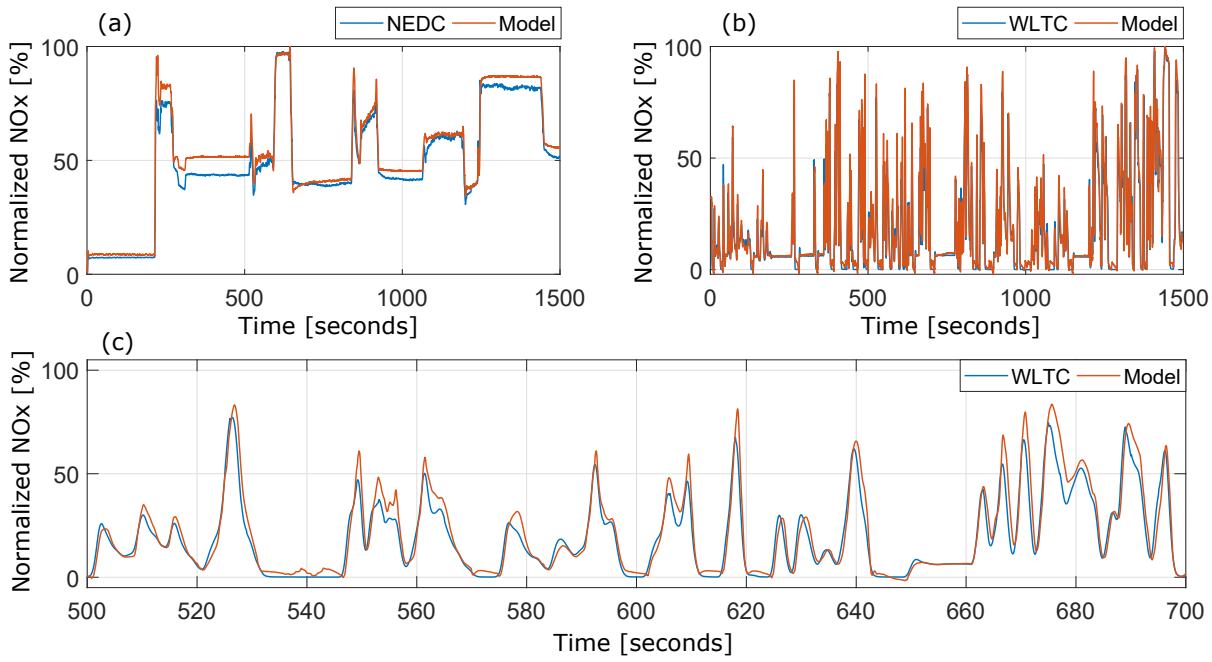

Figure 12: Validation performances of the model with 6 input regressors and 15 units (a) steady-state cycle (b) transient cycle, (c) zoomed-in version of transient cycle

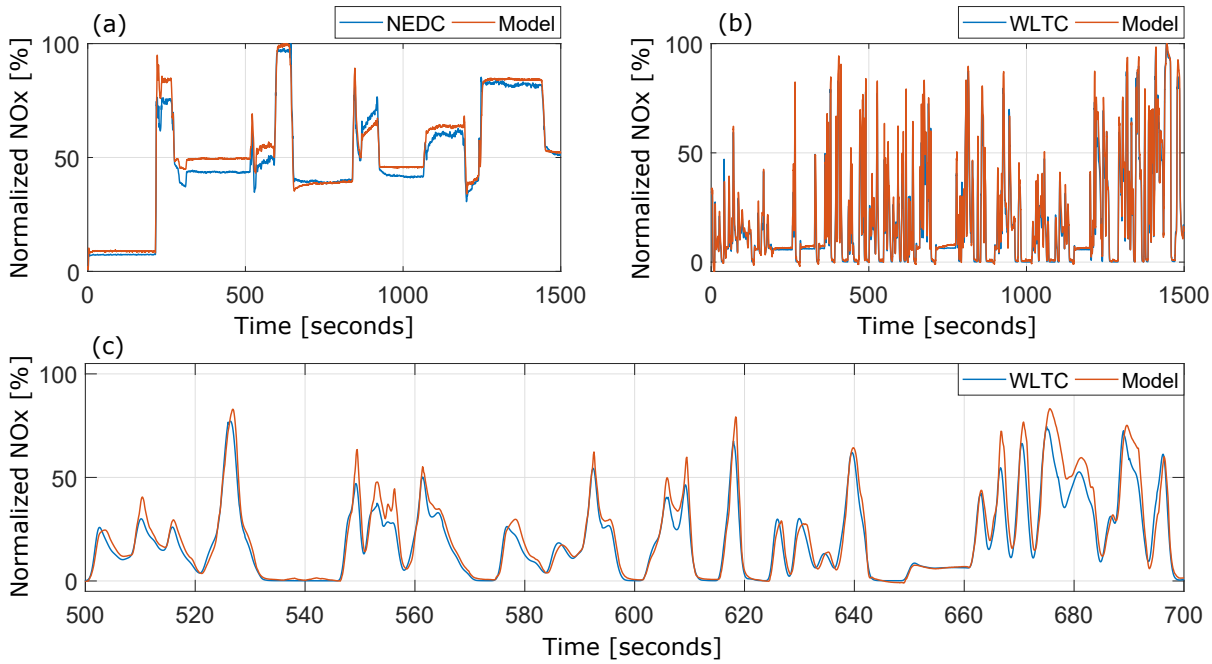

Figure 13: Validation performances of the model with 5 input regressors and 9 units (a) steady-state cycle (b) transient cycle, (c) zoomed-in version of transient cycle

Results in Figure 12, 13 and 14 show that the model predictions are very accurate in the transient regions of the validation tests compared to steady-state regions. It should be noted

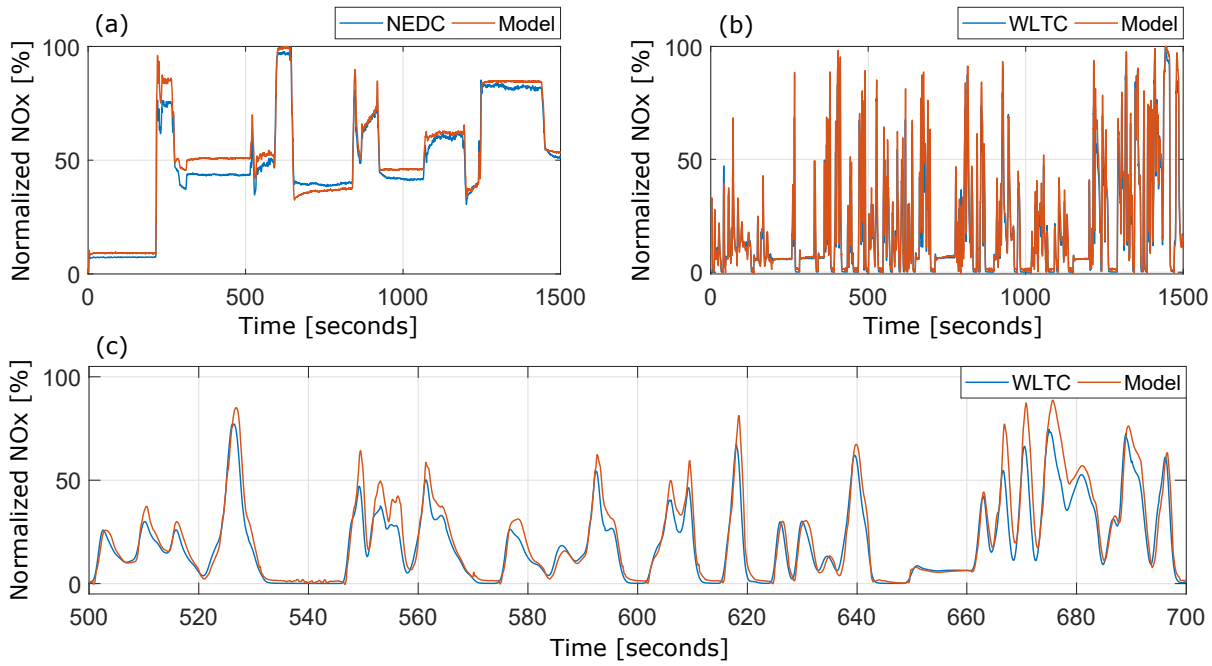

Figure 14: Validation performances of the model with 8 input regressors and 12 units (a) steady-state cycle (b) transient cycle, (c) zoomed-in version of transient cycle

that all of the input channels (except engine speed in Experiment 2) are excited by chirp signals during the training phase, which naturally enabled the model to learn the transient behavior properly. However, majority of the models still have the steady-state validation accuracy between 80%-90%. Indeed, it is still a challenging task to perform an experiment to model both steady-state and transient behavior of the diesel engine NOx emissions.

6. Conclusion

We have now presented a new design of experiment and nonlinear modeling of diesel engine NOx emissions based on sigmoid NARX models. In order to reduce the testing time and achieve high validation performances under both steady-state and transient cycles, all input channels were excited by chirp signals with quadratic changing frequencies. Moreover, correlations between inputs were lowered by selecting the number and the directions of the sweeps in frequency profiles differently to obtain maximum informative experiments. Sensitivity analysis of the models to parameter changes was conducted by generating models for different values of parameters and a parameter selection method using an easy-to-interpret map was proposed. The map can be a convenient means to select the required parameters

for diesel engine emissions modeling with limited testing time in powertrain development.

Training and validation results of the obtained models were quite promising. Majority of the models were trained with the fit accuracy higher than 80%. The steady-state and the transient validation accuracies of the selected best models were higher than 85% and 75%, respectively.

Steady-state and transient validation accuracies of selected best models are sufficiently accurate for calibration development purposes. Using these models, engineers can employ optimization routines to calibrate Fuel-Air control setpoint functions automatically. Since the purpose of the developed models is calibration optimization, having a model that offers a good sensitivity to variation in combustion inputs is very important. Currently, this model development process is not considered as a potential replacement for physical NOx sensors.

As a future work, we plan to develop strategies for reducing the offsets observed between the model predictions and the measurements during steady-state operations. The potential of the proposed modeling approach for NOx will also be investigated for soot emissions.

Acknowledgments

The funding provided by Ford Otosan is gratefully acknowledged.

References

[1] Hsieh, M. F., and Wang, J. NO and NO2 concentration modeling and observer-based estimation across a diesel engine aftertreatment system. *Journal of Dynamic Systems, Measurement, and Control*, 133(4), 041005, 2011.

[2] Sindhu, R., Rao, G. A. P., and Murthy, K. M. Effective reduction of NOx emissions from diesel engine using split injections. *Alexandria Engineering Journal*, 2017.

[3] Bertram, C., Rezaei, R., Tilch, B., and van Horrick, P. Development of an Euro VI engine using model-based calibration. *MTZ worldwide*, 75(10), 4–9, 2014.

[4] Stoev, J., and Schoukens, J. Nonlinear system identification - Application for industrial hydro-static drive-line. *Control Engineering Practice*, 54, 154–165, 2016.

[5] Rezaei, R., Dinkelacker, F., Tilch, B., Delebinski, T., and Brauer, M. Phenomenological modeling of combustion and NOx emissions using detailed tabulated chemistry methods in diesel engines. *International Journal of Engine Research*, 17(8), 846–856, 2016.

[6] Raptotasios, S. I., Sakellaridis, N. F., Papagiannakis, R. G., and Hountalas, D. T. Application of a multi-zone combustion model to investigate the NOx reduction potential of two-stroke marine diesel engines using EGR. *Applied Energy*, 157, 814–823, 2015.

[7] Perez, E., Blasco, X., Garcia-Nieto, S., and Sanchis, J. Diesel engine identification and predictive control using Wiener and Hammerstein models. *IEEE International Conference on Control Applications*, 2417–2423, 2006.

[8] Hirsch, M., Alberer, D., and Del Re, L. Grey-box control oriented emissions models. *IFAC Proceedings Volumes*, 41(2), 8514–8519, 2008.

[9] d'Ambrosio, S., Finesso, R., Fu, L., Mittica, A., and Spessa, E. A control-oriented real-time semi-empirical model for the prediction of NOx emissions in diesel engines. *Applied Energy*, 130, 265–279, 2014.

[10] Querel, C., Grondin, O., and Letellier, C. Semi-physical mean-value NO x model for diesel engine control. *Control Engineering Practice*, 40, 27–44, 2015.

[11] Asprion, J., Chinellato, O., and Guzzella, L. A fast and accurate physics-based model for the NO x emissions of Diesel engines. *Applied Energy*, 103, 221–233, 2013.

[12] Benatzky, C., Stadlbauer, S., Formentin, S., Schilling, A., and Alberer, D. Indicated pressure-based data-driven diesel engine NOx modeling. *International Journal of Engine Research*, 15(8), 934–943, 2014.

[13] Henningsson, M., Ekholm, K., Strandh, P., Tunestl, P., and Johansson, R. Dynamic mapping of diesel engine through system identification. *Identification for Automotive Systems*, 223–239, 2012.

[14] Grahn, M., Johansson, K., and McKelvey, T. Data-driven emission model structures for diesel engine management system development. *International Journal of Engine Research*, 15(8), 906–917, 2014.

[15] Formentin, S., Corno, M., Waschl, H., Alberer, D., and Savaresi, S. M. NOx Estimation in Diesel Engines via In-Cylinder Pressure Measurement. *IEEE Transactions on Control Systems Technology*, 22(1), 396–403, 2014.

[16] Boz, T., Unel, M., Yilmaz, V. A. M., Gurel, C., Bayburtlu, C., and Koprubasi, K. Diesel engine NOx emission modeling with airpath input channels. *Annual Conference of Industrial Electronics Society*, 003382–003387, 2015.

[17] Roy, S., Banerjee, R., and Bose, P. K. Performance and exhaust emissions prediction of a CRDI assisted single cylinder diesel engine coupled with EGR using artificial neural network. *Applied Energy*, 119, 330–340, 2014.

[18] Alcan, G., Unel, M., Aran, V., Yilmaz, M., Gurel, C., and Koprubasi, K. Diesel Engine NOx Emission Modeling Using a New Experiment Design and Reduced Set of Regressors. *IFAC-PapersOnLine*, 51(15), 168–173, 2018.

[19] ECE - United Nations, Regulation No. 83-07, 2015-02-04.

[20] Gurel, C., Ozmen, E., Yilmaz, M., Aydin, D., Koprubasi, K. Multi-Objective Optimization of Transient Air-Fuel Ratio Limitation of a Diesel Engine Using DoE Based Pareto-Optimal Approach. *SAE International Journal of Commercial Vehicles*, 10(2017-01-0587), 299–307, 2017.

[21] Stewart, G., Borrelli, F. A model predictive control framework for industrial turbodiesel engine control. *IEEE Conference on Decision and Control*, 5704–5711, 2008.

[22] Kitamura, Y., Mohammadi, A., Ishiyama, T., Shioji, M. Fundamental investigation of NOx formation in diesel combustion under supercharged and EGR conditions, (No. 2005-01-0364), *SAE Technical Paper*, 2005.

[23] Hametner, C., Stadlbauer, M., Deregnaucourt, M., Jakubek, S., Winsel, T. Optimal experiment design based on local model networks and multilayer perceptron networks. *Engineering Applications of Artificial Intelligence*, 26(1), 251–261, 2013.

[24] Pronzato, L. Optimal experimental design and some related control problems. *Automatica*, 44(2), 303–325, 2008.

[25] Santner, T. J., Williams, B. J., and Notz, W. I. *The design and analysis of computer experiments*, Springer Science and Business Media, 2013

[26] Ljung, L. *System Identification: Theory for the User*, Prentice Hall, 1999.

[27] Pintelon, R., and Schoukens, J. *System identification: a frequency domain approach*, John Wiley and Sons, 2012.

[28] Steven, H., Development of a worldwide harmonised heavy-duty engine emissions test cycle, Technical Report, United Nations, 2001.

[29] Barlow, T. J., Latham, S., McCrae, I. S., and Boulter, P. G. A reference book of driving cycles for use in the measurement of road vehicle emissions. TRL Published Project Report, 2009.

[30] Ljung, L. (2008). System Identification Toolbox 7: Getting Started Guide. The MathWorks.

[31] Ko, J., Jin, D., Jang, W., Myung, C. L., Kwon, S., and Park, S. Comparative investigation of NOx emission characteristics from a Euro 6-compliant diesel passenger car over the NEDC and WLTC at various ambient temperatures. *Applied energy*, 187, 652–662, 2017.